A 3D PATH-FOLLOWING VELOCITY-TRACKING CONTROLLER FOR AUTONOMOUS VEHICLES

Rita Cunha [*,1] **Carlos Silvestre** [*,2]

[*] *Instituto Superior Técnico,*
Institute for Systems and Robotics,
Av. Rovisco Pais, 1046-001 Lisboa, Portugal
{*rita,cjs*}*@isr.ist.utl.pt*

Abstract: This paper addresses the path-following problem of steering an autonomous vehicle along a desired path, while tracking a predefined velocity profile. The presented solution relies on the definition of a path-dependent error space to express the dynamic model of the vehicle, which is specially suited for a D-methodology controller implementation. The error space exhibits a high-degree of directionality accuracy in the definition of velocity references. The proposed strategy guarantees asymptotic stability of the closed-loop system about trimming paths, and has the particular feature of eliminating the need to feedforward trimming values for both actuation and vehicle orientation. The effectiveness of the technique is assessed in simulation with the full nonlinear model of a model-scale helicopter.

Keywords: Tracking Systems, Autonomous Vehicles, Implementation, Helicopter Control, Error Control

1. INTRODUCTION

In an ever increasing number of applications, autonomous vehicles are required to operate in challenging mission scenarios and uncertain environments. Consider, for example, the case of bridge inspections, where a camera-equipped helicopter is expected to follow complex three-dimensional paths to monitor the bridge pillars and deck and assess maintenance and repair requirements. Within the field of motion control for autonomous vehicles, the path-following approach arose as a response to the limitations of trajectory-tracking. Leading work in this area can be found in (Micaelli and Samson, 1993). In path-following, instead of tracking a time-parametrized reference, i.e., a trajectory, the vehicle is required to converge to and follow a path without temporal restrictions. Several examples show that, when compared to trajectory-tracking, path-following strategies consistently exhibit enhanced performance, with smoother convergence to the path and less demand on the control effort (Aguiar and Hespanha, 2004).

Reported solutions to the path-following problem rely mostly on nonlinear techniques including feedback linearization and Lyapunov-based design. The starting point of these approaches is the definition of a kinematic feedback control law for the angular velocity that converges to zero both the distance to the path and the angular displacement of the linear velocity vector, which is assumed not

[1] The work of R. Cunha was supported by a PhD Student Scholarship from the POCTI Programme of FCT, Portugal.
[2] This work was (partially) supported by the FCT POSI programme under framework QCA III and by the POSI/SRI/41938/2001 ALTICOPTER project.

to converge to zero. Initial solutions considered the kinematic model of a wheeled robot (Micaelli and Samson, 1993). This result has been extended in several aspects: the problem has been considered in three-dimensional space, as in (Encarnação and Pascoal, 2000), where a non-linear controller for underwater vehicles is proposed; kinematic control laws have been extended to account for vehicle dynamics and parameter uncertainty (Encarnação and Pascoal, 2000; Soeanto *et al.*, 2003; Aguiar and Hespanha, 2004). Typically, backstepping techniques are used to extend kinematic controllers to a dynamic setting. A major drawback of such methods is the fact that they are very restrictive on the structure of the vehicle's dynamic model.

In this paper, the path-following problem is addressed within the framework of the work reported in (Kaminer *et al.*, 1998; Silvestre *et al.*, 2002; Cunha *et al.*, 2003), while having in mind high-maneuverability vehicles, such as helicopters. The presented solution relies on the definition of a path-dependent error space to express the dynamic model of the vehicle. The error vector, which the path following controller should drive (partially or not) to zero, comprises velocity errors, orientation errors, and the distance to the path, defined as the distance between the vehicle's position and its orthogonal projection on the path.

Along the lines of the referred strategies, the current solution uses the fact the equilibrium points of the error dynamics correspond to trimming paths, comprising straight lines and z-aligned helices, and that the linearizations about such points are time-invariant. Therefore, the error space is specially suited for a D-methodology controller implementation (Kaminer *et al.*, 1995). This methodology ensures that the linearization of the nonlinear closed-loop system about the equilibrium points preserve the same internal as well as input-output properties of the corresponding linear closed loop designs. Moreover, the use of integral action guarantees zero steady-state error for the selected outputs and, since it is placed at the plant input, the need to feedforward trimming values for the actuation signals and outputs not required to track references is eliminated.

The main contribution of this paper is the definition of the error space itself. Due to a more accurate representation of error directionality, the proposed error space constitutes an improvement with respect to previous ones. In the definition of the reference velocity, instead of considering constant trimming values, the current vehicle orientation is taken into account. Moreover, the desired linear velocity is determined by the reference speed and distance to the path, so that it always points towards the path. These enhancements are particularly relevant for helicopters, since the angles of attack and sideslip may change substantially while following a path. Consider, for example, a maneuver including forward and vertical flight segments. In this respect, the present solution also extends the results of (Cunha *et al.*, 2003), since vertical flight maneuvers are now naturally included in the set of admissible paths.

The paper is organized as follows. Section 2 introduces the path following control problem for autonomous vehicles, describing the transformation applied to the vehicle dynamics to obtain an error dynamic model. Section 3 presents the controller implementation adopted and outlines its properties. Section 4 illustrates the application of the methodology to the specific case of model-scale helicopters. Concluding remarks are presented in Section 5.

2. PROBLEM FORMULATION

Consider a vehicle modeled as rigid-body, define $\{u\}$ as the inertial frame and $\{b\}$ as the body frame, attached to the vehicle's center of mass. Let $({}^u\mathbf{p}_b,\ {}^u_bR) \in SE(3) \triangleq \mathbb{R}^3 \times SO(3)$ denote the configuration of $\{b\}$ with respect to $\{u\}$ and $\boldsymbol{\lambda}_b = [\phi_b\ \theta_b\ \psi_b]',\ \theta_b \in\ ]-\pi/2, \pi/2[,\ \phi_b, \psi_b \in \mathbb{R}$ denote the Z-Y-X Euler angles, representing the orientation of $\{b\}$ relative to $\{u\}$. Consider also the linear and angular body velocities, $\mathbf{v}_b$ and $\boldsymbol{\omega}_b \in \mathbb{R}^3$, given respectively by $\mathbf{v}_b = {}^b_uR\,{}^u\dot{\mathbf{p}}_b$ and $\boldsymbol{\omega}_b = {}^b_uR\,{}^u\boldsymbol{\omega}_b$, where ${}^u\boldsymbol{\omega}_b \in \mathbb{R}^3$ is the angular velocity of $\{b\}$ with respect to $\{u\}$. Then, the vehicle's kinematics can be described by

$$\begin{cases} {}^u\dot{\mathbf{p}}_b = {}^u_bR\,\mathbf{v}_b \\ \dot{\boldsymbol{\lambda}}_b = Q(\phi_b,\, \theta_b)\,\boldsymbol{w}_b \end{cases}, \tag{1}$$

where

$$Q(\phi_b,\, \theta_b) = \begin{bmatrix} 1 & \sin\phi_b \tan\theta_b & \cos\phi_b \tan\theta_b \\ 0 & \cos\phi_b & -\sin\phi_b \\ 0 & \sin\phi_b/\cos\theta_b & \cos\phi_b/\cos\theta_b \end{bmatrix}, \tag{2}$$

and the derivative of ${}^u_bR$ is given by ${}^u_b\dot{R} = {}^u_bR\,S(\boldsymbol{\omega}_b)$, where $S(x) \in \mathbb{R}^{3\times3}$ is a skew symmetric matrix such that $S(x)\,y = x \times y$, for all x, $y \in \mathbb{R}^3$. Based on the Newton-Euler equations, the dynamic model of the vehicle can be written as

$$\begin{cases} m\dot{\mathbf{v}}_b = \mathbf{f}(\mathbf{v}_b, \boldsymbol{\omega}_b, \mathbf{u}) + m^b_uR[0\ 0\ g]' - S(\boldsymbol{\omega}_b)m\mathbf{v}_b \\ I\dot{\boldsymbol{\omega}}_b = \mathbf{n}(\mathbf{v}_b, \boldsymbol{\omega}_b, \mathbf{u}) - S(\boldsymbol{\omega}_b)I\boldsymbol{\omega}_b \end{cases}, \tag{3}$$

where $m \in \mathbb{R}$ and $I \in \mathbb{R}^{3\times3}$ denote the vehicle mass and moment of inertia, respectively; g denotes the gravitational acceleration; and $\mathbf{f}$, $\mathbf{n}$: $(\mathbb{R}^3, \mathbb{R}^3, \mathbb{R}^{n_u}) \to \mathbb{R}^3$ represent the external forces and moments acting on the body, which are in general continuously differentiable functions of the body velocities and control inputs $\mathbf{u} \in \mathbb{R}^{n_u}$.

2.1 Error space definition

The objective of the feedback control law to be defined consists in steering the vehicle along a

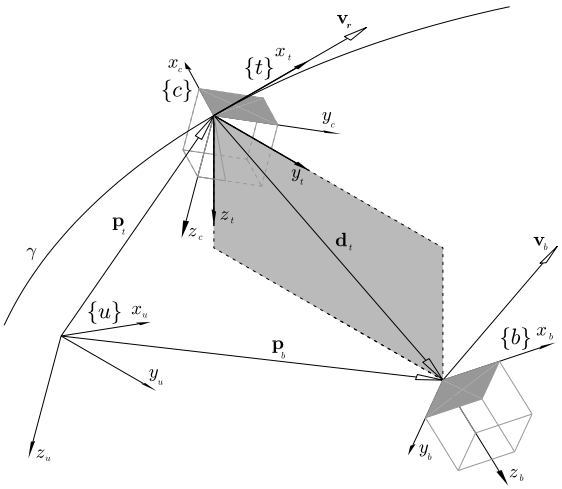

Fig. 1. Coordinate frames: inertial $\{u\}$, body $\{b\}$, tangent $\{t\}$, and desired body frame $\{c\}$

desired path, which corresponds to a smooth three-dimensional curve γ, parametrized by a scalar, such as the arc-length s. Then, for each point in γ, one can define the curvature $\kappa(s) \geq 0$, the torsion $\tau(s) \in \mathbb{R}$, and the tangent frame $\{t\}$, also known as Serret-Frenet frame, with orientation ${}^u_t R = [\mathbf{t}(s)\ \mathbf{n}(s)\ \mathbf{b}(s)] \in SO(3)$ consisting of the tangent, normal, and binormal vectors, respectively. In the following, the dependence on s is omitted, for reasons of simplicity. From the definition of $\{t\}$, it follows that: *i)* the linear velocity $\mathbf{v}_t = {}^t_u R\, {}^u\dot{\mathbf{p}}_t \in \mathbb{R}^3$ takes the form $\mathbf{v}_t = V_t[1\ 0\ 0]$ where $V_t \in \mathbb{R}$ gives the speed with which the tangent frame is moving along the curve, i.e., $V_t = \dot{s}$; *ii)* according to the Serret-Frenet formulas, the motion of ${}^u_t R$ is ruled by ${}^u_t\dot{R} = V_t\, {}^u_t R\, S([\tau\ 0\ \kappa]')$; and *iii)* the angular velocity $\boldsymbol{\omega}_t = {}^t_u R\, {}^u\boldsymbol{\omega}_t$ is therefore given by $\boldsymbol{\omega}_t = V_t[\tau\ 0\ \kappa]'$.

The vehicle's dynamics will be expressed in a path-dependent error space, whose definition relies heavily on the tangent frame $\{t\}$. The underlying idea consists in constraining the tangent frame's motion to depend on the body's motion, such that the origin of $\{t\}$ coincides with the point in γ closest to the vehicle, or, in other words, such that the distance vector $\mathbf{d} = {}^u\mathbf{p}_b - {}^u\mathbf{p}_t$ is perpendicular to γ, see Figure 1. Then, the body position can be expressed in terms of the arc-length s and the distance vector $\mathbf{d}_t = [d_y\ d_z]' \in \mathbb{R}^2$ that verifies ${}^t_u R\,\mathbf{d} = [0\ \mathbf{d}_t']'$. Simple manipulations show that the speed of the tangent frame is given by

$$\dot{s} = V_t = \frac{1}{1 - \kappa\, d_y} \begin{bmatrix} 1 & 0 & 0 \end{bmatrix} {}^t_b R\, \mathbf{v}_b \qquad (4)$$

and that the motion of $\mathbf{d}_t$ is ruled by

$$\dot{\mathbf{d}}_t = V_t \tau \begin{bmatrix} 0 & 1 \\ -1 & 0 \end{bmatrix} \mathbf{d}_t + \begin{bmatrix} 0 & 1 & 0 \\ 0 & 0 & 1 \end{bmatrix} {}^t_b R\, \mathbf{v}_b. \qquad (5)$$

In order to ensure that a vehicle not only follows a predefined curve γ but also tracks a given velocity profile and keeps a certain orientation, extra references are needed. For that purpose, consider the reference tangent speed V_r and angular velocity $\boldsymbol{\omega}_r = \frac{V_r}{V_t}\boldsymbol{\omega}_t$. In addition, define $\{c\}$ as the desired body frame that moves together with $\{t\}$, but with the desired body orientation, see Fig. 1. The need to define $\{c\}$ arises from the fact that while following a path and keeping the desired speed V_r along the path, the vehicle may take different orientations or even rotate with respect to the path. The desired orientation given by the Z-Y-X Euler angles $\boldsymbol{\lambda}_c = [\phi_c\ \theta_c\ \psi_c]'$, $\theta_c \in\,]-\pi/2, \pi/2[\,$, $\phi_c, \psi_c \in \mathbb{R}$ and the relative angular velocity ${}^t\boldsymbol{\omega}_c \in \mathbb{R}^3$ provide these references. Notice that the derivative of $\boldsymbol{\lambda}_c$ can be written as $\dot{\boldsymbol{\lambda}}_c = Q(\phi_c, \theta_c)\, {}^c_t R\, (\boldsymbol{\omega}_t + {}^t\boldsymbol{\omega}_c)$.

Given the definitions of $\{t\}$, $\{c\}$, and references V_r and $\boldsymbol{\omega}_r$, consider the following error state vector

$$\mathbf{x}_e = \begin{bmatrix} \mathbf{v}_e \\ \boldsymbol{\omega}_e \\ \mathbf{d}_t \\ \boldsymbol{\lambda}_e \end{bmatrix} = \begin{bmatrix} \mathbf{v}_b - {}^b_t R\, [V_r\ -\mathbf{d}_t']' \\ \boldsymbol{\omega}_b - {}^b_t R\, (\boldsymbol{\omega}_r + {}^t\boldsymbol{\omega}_c) \\ \mathbf{d}_t \\ \boldsymbol{\lambda}_b - \boldsymbol{\lambda}_c \end{bmatrix} \in \mathbb{R}^{11}. \quad (6)$$

It is straightforward to verify that the vehicle follows a path γ with speed $V_t = V_r$, relative angular velocity ${}^t\boldsymbol{\omega}_b = {}^t\boldsymbol{\omega}_c$, and orientation $\boldsymbol{\lambda}_b = \boldsymbol{\lambda}_c$ if and only if $\mathbf{x}_e = 0$.

It should be noted that the reference velocities are determined in the tangent frame $\{t\}$ and then rotated to the current body frame $\{b\}$. This is in contrast with previous approaches (Kaminer *et al.*, 1998; Cunha *et al.*, 2003), where the references were rotated to $\{c\}$ instead of $\{b\}$. With a significant orientation error, directionality of the velocity errors could be lost. In the current approach, the velocity errors $\mathbf{v}_e$ and $\boldsymbol{\omega}_e$ do not depend on the orientation error, so that keeping $\boldsymbol{\lambda}_e \neq 0$ while the remaining error components are driven to zero, still ensures that the vehicle follows the path with the desired speed, but now with arbitrary orientation. In addition, instead of setting the reference body velocity to be tangent to the path, i.e. $\mathbf{v}_e = \mathbf{v}_b - {}^b_t R[V_r\ 0\ 0]'$, the distance to the path is taken into account, so that the desired velocity always points towards the path, i.e. $\mathbf{v}_e = \mathbf{v}_b - {}^b_t R[V_r\ -\mathbf{d}_t']'$.

2.2 Error dynamics

Until now, it has been assumed that γ can be any smooth 3-D space curve to be followed with arbitrary velocity and orientation. The set of allowable paths will hereafter be restricted to that of the so-called trimming paths. Similarly, the reference speed V_r and the motion of $\{c\}$ will correspond to trimming trajectories consistent with the chosen path. A trimming path corresponds to a curve that the vehicle can follow while satisfying the trimming condition, which is equivalent to having $\dot{\mathbf{v}}_b = 0$, $\dot{\boldsymbol{\omega}}_b = 0$, and $\dot{\mathbf{u}} = 0$ in (3). It is well known that, for a vehicle with dynamics described by (3) and assuming constant gravitational acceleration,

the set of trimming trajectories comprises all z-aligned helices ($\dot{\kappa}=0$, $\dot{\tau}=0$, $\boldsymbol{\lambda}_t=[0\ \theta_t\ \psi_t]'$, and $\dot{\boldsymbol{\lambda}}_t = V_t\sqrt{\kappa^2+\tau^2}\,[0\ 0\ 1]'$), followed at constant speed ($\dot{V}_t=0$) and constant orientation relative to the path (${}^t\boldsymbol{\omega}_c=0$). For helices, the flight path angle θ_t is given by $\theta_t=\arctan(-\tau/\kappa)$, while in the case of straight lines ($\kappa=0$, $\tau=0$), θ_t is a predefined constant. The following set of constraints can therefore be imposed on the reference path and velocities: $\dot{V}_r=0$, $\dot{\kappa}=0$, $\dot{\tau}=0$, ${}^t\boldsymbol{\omega}_c=0$, and $\dot{\boldsymbol{\lambda}}_c = V_t\sqrt{\kappa^2+\tau^2}\,[0\ 0\ 1]'$.

Under these constraints, the error dynamics can be written as

$$\begin{cases} \dot{\mathbf{v}}_e = \dot{\mathbf{v}}_b + S(\boldsymbol{\omega}_e)\,{}^b_tR\begin{bmatrix} V_r \\ -\mathbf{d}_t\end{bmatrix} + \mathbf{v}_e \\ \qquad\quad + {}^b_tR\,(S(\boldsymbol{\omega}_r)+I_3)\begin{bmatrix} V_r - V_t \\ -\mathbf{d}_t\end{bmatrix} \\ \dot{\boldsymbol{\omega}}_e = \dot{\boldsymbol{\omega}}_b - S(\boldsymbol{\omega}_e)\,{}^b_tR\,\boldsymbol{\omega}_r \\ \dot{\mathbf{d}}_t = \left(V_t\tau\begin{bmatrix}0 & 1\\ -1 & 0\end{bmatrix} - I_2\right)\mathbf{d}_t + \begin{bmatrix}0 & 1 & 0\\ 0 & 0 & 1\end{bmatrix}{}^t_bR\,\mathbf{v}_e \\ \dot{\boldsymbol{\lambda}}_e = Q(\phi_b,\,\theta_b)\boldsymbol{\omega}_b - V_t\sqrt{\kappa^2+\tau^2}[0\ 0\ 1]' \end{cases}, \quad (7)$$

with $\dot{\mathbf{v}}_b$ and $\dot{\boldsymbol{\omega}}_b$ given by (3) and V_t by (4). Notice that the gravitational term in (3) can be written as ${}^b_uR\,[0\ 0\ g]' = R_x(\phi_b)'R_y(\theta_b)'[0\ 0\ g]'$ and that ${}^t_bR = R_y(\theta_t)'R_z(\psi_{ct}+\psi_e)R_y(\theta_b)R_x(\phi_b)$, where ψ_{ct} denotes the constant difference $\psi_c - \psi_t$. Thus, the need to include the arc-length s in the state vector is eliminated, since the only terms that depend explicitly on s, ψ_b and ψ_c, do not appear isolated. Consider the parameter vector $\boldsymbol{\xi} = (V_r,\,\dot{\psi}_r,\,\theta_t,\,\phi_c,\,\theta_c,\,\psi_{ct})$, where $\dot{\psi}_r = V_r\sqrt{\kappa^2+\tau^2}$ denotes the reference yaw rate. It is easy to verify that, apart from a translation or a z-axis rotation, $\boldsymbol{\xi}$ completely characterizes a trimming trajectory. Then, the system consisting of (7) and an output signal $\mathbf{y}$ can be written in compact form as

$$\mathcal{P} := \begin{cases} \dot{\mathbf{x}}_e = \mathbf{f}_1(\mathbf{x}_e,\boldsymbol{\xi}) + \mathbf{f}_2(\mathbf{v}_b,\,\boldsymbol{\omega}_b,\mathbf{u}) \\ \mathbf{y} = \mathbf{g}(\mathbf{x}_e,\boldsymbol{\xi}) \end{cases}, \quad (8)$$

where the output function satisfies $\mathbf{g}(0,\boldsymbol{\xi})=0$ and, according to (6), the body velocities $\mathbf{v}_b$ and $\boldsymbol{\omega}_b$ are explicit functions of $\mathbf{x}_e$ and $\boldsymbol{\xi}$. The following result shows that all trimming trajectories correspond to equilibrium points of the error system (8).

Proposition 1. Consider a reference parametrization denoted by $\boldsymbol{\xi}_0 = (V_r,\,\dot{\psi}_r,\,\theta_t,\,\phi_c,\,\theta_c,\,\psi_{ct})$. Define $\mathbf{u}_0$ as a constant vector that satisfies (3) with $\mathbf{v}_b = {}^c_tR\,\mathbf{v}_r$, $\boldsymbol{\omega}_b = {}^c_tR\,\boldsymbol{\omega}_r$, ($\dot{\mathbf{v}}_b = \dot{\boldsymbol{\omega}}_b = 0$), $\phi_b=\phi_c$, and $\theta_b=\theta_c$. Then $\mathbf{x}_e=0$ is an equilibrium point of (8), when $\boldsymbol{\xi}=\boldsymbol{\xi}_0$ and $\mathbf{u}=\mathbf{u}_0$.

PROOF. The proof follows from direct substitutions of the equilibrium point in the appropriate equations. If $\mathbf{x}_e=0$, then, by (6), $\mathbf{v}_b = {}^c_tR\,\mathbf{v}_r$, $\boldsymbol{\omega}_b = {}^c_tR\,\boldsymbol{\omega}_r$, $\boldsymbol{\lambda}_b = \boldsymbol{\lambda}_c$, and, by (4), $V_t = V_r$. Given the definition of $\mathbf{u}_0$, it follows that $\dot{\mathbf{v}}_b = 0$ and $\dot{\boldsymbol{\omega}}_b = 0$. Using these results in (7) yields $\dot{\mathbf{v}}_e = 0$, $\dot{\boldsymbol{\omega}}_e = 0$, $\dot{\mathbf{d}}_t = 0$, and $\dot{\boldsymbol{\lambda}}_e = Q(\phi_c,\,\theta_c)\,{}^c_tR\,\boldsymbol{\omega}_r - V_r\sqrt{\kappa^2+\tau^2}[0\ 0\ 1]'$. Simple algebraic manipulations show that $\dot{\boldsymbol{\lambda}}_e = 0$.

Using the above defined error space, the path-following problem initially proposed, i.e., that of steering the vehicle along a path with a certain velocity and orientation profile, can be formulated as follows:

Problem 2. Given a set of reference parametrizations $\Xi = \left\{\boldsymbol{\xi} = (V_r,\,\dot{\psi}_r,\,\theta_t,\,\phi_c,\,\theta_c,\,\psi_{ct})\right\}$, design a feedback control law for $\mathbf{u}$ such that, for each $\boldsymbol{\xi}_0\in\Xi$, the error system (8) is asymptotically stabilized about the corresponding equilibrium point.

As a result of this formulation, the desired paths to be considered may consist of a piece-wise continuous concatenation of trimming paths. The design methodology adopted to solve Problem 2 involves obtaining the linearization of (8) about ($\mathbf{x}_e = 0$, $\boldsymbol{\xi}=\boldsymbol{\xi}_0$, $\mathbf{u}=\mathbf{u}_0$), for each $\boldsymbol{\xi}_0\in\Xi$. It is straightforward to verify that such linearizations result in linear time-invariant systems described by

$$\mathcal{P}_l(\boldsymbol{\xi}_0) := \begin{cases} \delta\dot{\mathbf{x}}_e = A(\boldsymbol{\xi}_0)\delta\mathbf{x}_e + B_1(\boldsymbol{\xi}_0)\delta\boldsymbol{\xi} + B_2(\boldsymbol{\xi}_0)\delta\mathbf{u} \\ \delta\mathbf{y} = C(\boldsymbol{\xi}_0)\delta\mathbf{x}_e + D(\boldsymbol{\xi}_0)\delta\boldsymbol{\xi} \end{cases}. \quad (9)$$

Analytical expressions for the $\boldsymbol{\xi}_0$-dependent coefficient matrices can be found in (Cunha and Silvestre, 2004).

3. CONTROLLER DESIGN AND IMPLEMENTATION

The controller implementation adopted to solve the path-following problem relies on the so-called D-methodology, see (Silvestre *et al.*, 2002) and references therein. The first step of this method consists in designing linear controllers, for the family of linear systems $\mathcal{P}_l(\boldsymbol{\xi}_0)$, $\boldsymbol{\xi}_0\in\Xi$. In this paper, it is assumed that a single state feedback linear controller $\mathcal{C}_l$, with integral action on the output, of the form

$$\mathcal{C}_l := \begin{cases} \delta\dot{\mathbf{x}}_c = \delta\mathbf{y} \\ \delta\mathbf{u} = K_1\delta\mathbf{x}_e + K_2\delta\mathbf{x}_c \end{cases}, \quad (10)$$

can be synthesized, such that, for all $\boldsymbol{\xi}_0\in\Xi$, the closed-loop system consisting of (9-10) is asymptotically stable and zero steady-state error for $\mathbf{y}$ is achieved. Given $\mathcal{C}_l$, the D-methodology controller for the nonlinear system (8) is implemented as follows,

$$\mathcal{C} := \begin{cases} \dot{\mathbf{x}}_c = K_1\dot{\mathbf{x}}_e + K_2\mathbf{y} \\ \mathbf{u} = \mathbf{x}_c \end{cases}. \quad (11)$$

The D-methodology exhibits a fundamental *linearization property*, which can be described as follows: assume that $\dim(\mathbf{x}_c) = \dim(\mathbf{y})$, K_2 is invertible, and $\mathbf{y}_0 = \mathbf{g}(0, \boldsymbol{\xi}_0) = 0$, for each $\boldsymbol{\xi}_0 \in \Xi$, then the linearization of the closed-loop system consisting of $\mathcal{P}$ and $\mathcal{C}$ about $(\mathbf{x}_e = 0, \boldsymbol{\xi} = \boldsymbol{\xi}_0, \mathbf{u} = \mathbf{u}_0)$ and the linear closed-loop system formed by $\mathcal{P}_l(\boldsymbol{\xi}_0)$ and $\mathcal{C}_l$ have the same internal and input-output properties (Kaminer *et al.*, 1995).

Alongside the already stated linearization property, the D-methodology implementation has other important features, which are worthwhile emphasizing: i) *auto-trimming property* - the controller automatically generates adequate trimming values for the actuation signals and for the state variables that are not required to track reference inputs; ii) the implementation of anti-windup schemes is straightforward, due to the placement of the integrators at the plant input.

4. EXAMPLE: PATH-FOLLOWING CONTROL FOR A MODEL-SCALE HELICOPTER

This section illustrates the application of the methodology just introduced to the design of a path-following controller for an autonomous model-scale helicopter. After a brief description of the design steps, simulation results for the closed-loop system are presented.

The controller was designed and implemented using *SimModHeli* (Cunha and Silvestre, 2003), a dynamic simulation model specially suited for model-scale helicopters. *SimModHeli* was derived from first-principles and has the particular feature of modeling the Bell-Hiller stabilizing bar, a mechanical device that improves helicopter stability and has become a standard in model-scale helicopters. The dynamics of the helicopter is described using the rigid body model (1-3), driven by forces and moments that explicitly include the effects of the main rotor, Bell-Hiller stabilizing bar, tail rotor, fuselage, horizontal tailplane, and vertical fin. The control inputs are given by $\mathbf{u} = [\delta_0 \ \delta_{1c} \ \delta_{1s} \ \delta_{0t}]'$, where δ_0 is the main rotor collective input, δ_{1c} and δ_{1s} the cyclic inputs for main rotor and Bell-Hiller flybar, and δ_{0t} the tail rotor collective input.

The first design step consists in defining an output signal $\mathbf{y}$, with the same dimension as $\mathbf{u}$, to be driven to zero at steady-state. The following output was considered $\mathbf{y} = [\mathbf{v}_e' \ \psi_e]'$. By including $\mathbf{v}_e$ in $\mathbf{y}$, both the velocity and position errors are being considered (recall the definition of $\mathbf{v}_e$), with the distance vector expressed in the current body frame. The choice of ψ_e as the remaining output arises from the specific characteristics of the helicopter. It can be shown that a helicopter may describe a trimming trajectory with arbitrary but constant yaw angle, with respect to the path being followed, automatically constraining the roll and pitch angles. Then, including ψ_e in $\mathbf{y}$ is a natural choice, since it completely determines the reference orientation of the vehicle and allows, for example, the same path to be followed forward or sideways.

The design procedure ensues with the selection of a family of equilibrium points Ξ, consistent with the reference path and velocities. In the present example, the desired path was selected so as to reflect the maneuvers involved in a bridge inspection operation. It is divided in four segments: i) level flight along the x-axis, ii) climbing helix; iii) positive ramp in the *yoz* plane; and iv) vertical climbing flight. The parameters and initial position of each stage are presented in Table 1. The reference ψ_{ct} is set to $\pi/2$, assigning a sideways motion for the first three stages of the path.

Table 1. Reference path parameters

V_r(m/s)	$\dot{\psi}_r$(rad/s)	θ_t(rad)	$\mathbf{p}_0$(m)
2	0	0	$[\ 0\ \ 0\ \ \ 0]'$
2	$3/40\pi$	0.34	$[20\ \ 0\ \ \ 0]'$
1	0	$5/6\pi$	$[12\ \ 8{-}13.4]'$
1	0	$\pi/2$	$[12{-}8{-}20.8]'$

Given the linearized systems $\mathcal{P}_l(\boldsymbol{\xi}_0)$, an LMI approach was used to solve an $\mathcal{H}_2$-type state-feedback problem (Ghaoui and Niculescu, 1999) and obtain a linear controller $\mathcal{C}_l$ as given in (10), ensuring asymptotic stability of the closed-loop system formed by $\mathcal{P}_l(\boldsymbol{\xi}_0)$ and $\mathcal{C}_l$, for all $\boldsymbol{\xi}_0 \in \Xi$. The corresponding D-methodology controller is simply obtained from (11). As depicted in Fig. 2, block Π is responsible for the computation of the closest orthogonal projection of $\mathbf{p}_b$ on the desired path segments described by Ξ, so as to determine the current values for $\mathbf{d}_t$, ${}^u_t R$, and path parameters V_r, κ, and τ. The error vector derivative $\dot{\mathbf{x}}_e$ and output $\mathbf{y} = [\mathbf{v}_e' \ \psi_e]'$ can then be obtained, according to (7) and (6), respectively. It now becomes clear that given the error space structure and choice of outputs, the adopted controller implementation eliminates the need to feedforward the trimming values for roll and pitch, ϕ_c and θ_c, respectively.

Simulation results were obtained using the nonlinear dynamic model *SimModHeli*, parametrized for the Vario X-Treme model-scale helicopter. The path described by the helicopter and corresponding actuation signals are shown in Figures 3 and 4, respectively. Figure 5 depicts the components

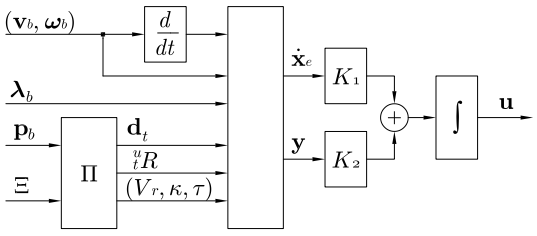

Fig. 2. D-methodology controller implementation

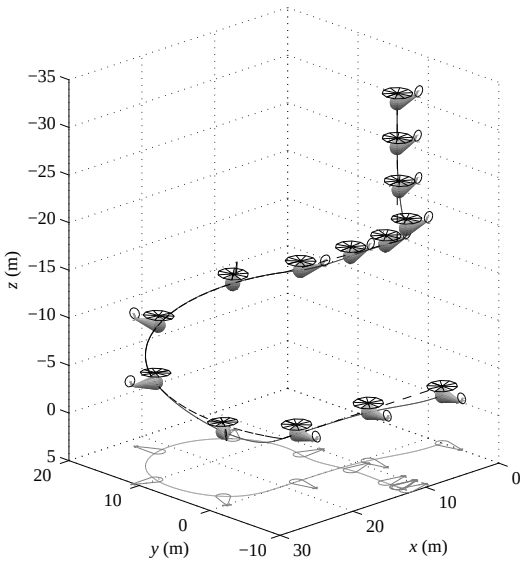

Fig. 3. Reference path (dashed), observed path (solid), and projection on xoy plane (gray)

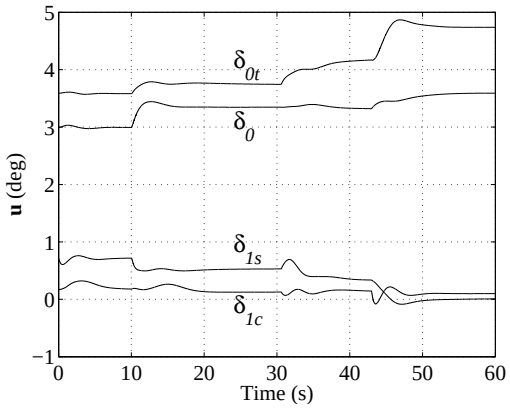

Fig. 4. Control activity: main rotor collective (δ_0), cyclics (δ_{1c}, δ_{1s}), and tail rotor collective (δ_{0t})

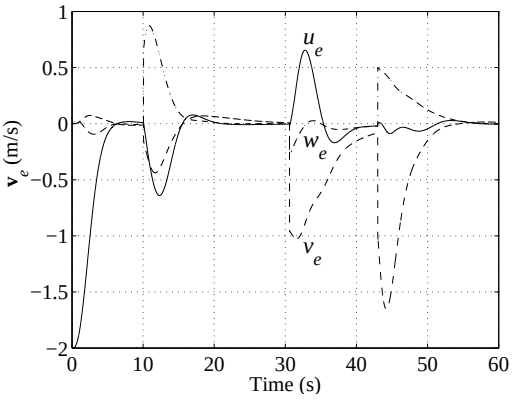

Fig. 5. Linear velocity errors: $\mathbf{v}_e = [u_e \; v_e \; w_e]'$

of $\mathbf{v}_e$, reflecting their dependence on the position errors. As shown in Figure 3, the initial position was perturbed from the origin to $\mathbf{p}_0 = [0 \; -2 \; 0]'$ m. The helicopter quickly converges to the reference path (dashed line) and stays on track through the remainder of the simulation. Only slight deviations occur, during the transition between stages.

5. CONCLUSION

This paper described a methodology for the design of path-following systems for autonomous vehicles. The presented solution builds on the definition of a new path-dependent error-space, which renders the velocity errors independent from the desired vehicle orientation and considers not only a reference speed but also the distance to the path when defining the reference linear velocity. Controller implementation relied on the D-methodology. A simulation example applied to model-scale helicopters illustrated the performance of the proposed path-following controller.

REFERENCES

Aguiar, P. and J. Hespanha (2004). Trajectory-tracking and path-following of underactuated autonomous vehicles with parametric modeling uncertainty. Submitted to IEEE TAC.

Cunha, R. and C. Silvestre (2003). Dynamic modeling and stability analysis of model-scale helicopters with bell-hiller stabilizing bar. In: *AIAA Guidance, Navigation, and Control Conference*.

Cunha, R. and C. Silvestre (2004). Path-following velocity-tracking control for autonomous vehicles. Technical report. ISR-IST.

Cunha, R., C. Silvestre and A. Pascoal (2003). A path following controller for model-scale helicopters. In: *European Control Conference*.

Encarnação, P. and A. Pascoal (2000). 3D path following for autonomous underwater vehicle. In: *39th IEEE Conference on Decision and Control*. pp. 2977–2982.

Ghaoui, L. El and Niculescu, S. I., Eds.) (1999). *Advances in Linear Matrix Inequality Methods in Control*. SIAM. Philadelphia.

Kaminer, I., A. Pascoal, E. Hallberg and C. Silvestre (1998). Trajectory tracking for autonomous vehicles: An integrated approach to guidance and control. *AIAA Journal of Guidance, Control, and Dynamics* **21**(1), 29–38.

Kaminer, I., A. Pascoal, P. Khargonekar and E. Coleman (1995). A velocity algorithm for the implementation of gain-scheduled controllers. *Automatica* **31**(8), 1185–1191.

Micaelli, A. and C. Samson (1993). Trajectory tracking for unicycle-type and two-steering-wheels mobile robots. Technical Report 2097. INRIA.

Silvestre, C., A. Pascoal and I. Kaminer (2002). On the design of gain-scheduled trajectory tracking controllers. *International Journal of Robust and Nonlinear Control* **12**, 797–839.

Soeanto, D., L. Lapierre and A. Pascoal (2003). Adaptive non-singular path-following, control of dynamic wheeled robots. In: *11th International Conference on Advanced Robotics*. pp. 1387–1392.